Physics of Plasmas

LETTER | OCTOBER 16 2025

The role of x-ray self-absorption effects in plasma generated by double-sided irradiation of foil targets with femtosecond laser pulses

I. Yu. Skobelev ; M. A. Alkhimova ; T. Pikuz; S. N. Ryazantsev ; R. K. Kulikov; A. Sagisaka; K. Ogura; Ko. Kondo ; Y. Miyasaka; M. Nishikino ; M. Kando ; H. Kiriyama; A. S. Pirozhkov ; K. Kondo; M. Ota; S. Egashira; T. Minami ; S. Jinno ; M. Kanasaki ; Y. Kuramitsu ; T. Kawachi ; R. Kodama; Y. Fukuda ; S. Pikuz ; Y. Sakawa

Phys. Plasmas 32, 100704 (2025)
https://doi.org/10.1063/5.0282642

Physics of Plasmas LETTER pubs.aip.org/aip/pop

The role of x-ray self-absorption effects in plasma generated by double-sided irradiation of foil targets with femtosecond laser pulses

Cite as: Phys. Plasmas **32**, 100704 (2025); doi: 10.1063/5.0282642
Submitted: 27 May 2025 · Accepted: 29 September 2025 ·
Published Online: 16 October 2025

I. Yu. Skobelev,[1,2] M. A. Alkhimova,[1,2] T. Pikuz,[3] S. N. Ryazantsev,[1,2,a)] R. K. Kulikov,[1,2] A. Sagisaka,[4] K. Ogura,[4] Ko. Kondo,[4] Y. Miyasaka,[4] M. Nishikino,[4] M. Kando,[4] H. Kiriyama,[4] A. S. Pirozhkov,[4] K. Kondo,[4] M. Ota,[5,6] S. Egashira,[5] T. Minami,[4,7] S. Jinno,[8] M. Kanasaki,[9] Y. Kuramitsu,[7] T. Kawachi,[4] R. Kodama,[5,7] Y. Fukuda,[4] S. Pikuz,[10] and Y. Sakawa[5]

AFFILIATIONS

[1]National Research Nuclear University MEPHI, Moscow, Russia
[2]Joint Institute for High Temperature RAS, Moscow, Russia
[3]Institute for Open and Transdisciplinary Research Initiatives, Osaka University, Osaka, Japan
[4]Kansai Institute for Photon Science, QST, Kizugawa, Kyoto, Japan
[5]Institute of Laser Engineering, Osaka University, Osaka, Japan
[6]National Institute for Fusion Science, Toki City, Gifu, Japan
[7]Graduate School of Engineering, Osaka University, Osaka, Japan
[8]Nuclear Professional School, The University of Tokyo, 2-22 Shirakata Shirane, Tokai-mura, Naka-gun 319-1188, Ibaraki, Japan
[9]Graduate School of Maritime Sciences, 5-1-1 Fukae-Minamimachi, Higashinada-Ku, Kobe 658-0022, Hyogo, Japan
[10]HB11 Energy Holdings, Freshwater, New South Wales, Australia

[a)]**Author to whom correspondence should be addressed:** ryazantsev.serj@gmail.com

ABSTRACT

In relativistic plasma expansion, a relative motion of plasma components causes absorption of spectral lines to be Doppler-shifted with respect to the emission line centers. The shift of spectral line can be of an order or exceeding the natural linewidth, leading to a significant reduction in self-absorption and optical thickness of the plasma. In this paper we experimentally examine the effect of femtosecond relativistic laser plasma expanding from both sides of the solid foil target. In an experiment, a hot plasma x-ray source in a 1–2 μm thin 4-chlorostyrene foil was created by high-contrast $\sim 1 \times 10^{21}$ W/cm^2 pulses delivered by the J-KAREN-P facility. In addition, the rear side of the target was heated by 1/100 of the main pulse power with a controlled few-nanosecond time delay. It is demonstrated that the high velocity of the downstream and upstream (from the rear side) plasma expansion essentially induces plasma transparency for K-shell emission from He-like chlorine ions dominating the ion charge distribution.

INTRODUCTION

When a laser pulse interacts with matter, the energy absorbed directly in the interaction region is distributed over the volume of the laser target due to several mechanisms.[1–3] As a result, ionization of the target matter atoms up to highly charged states occurs not only within the focal spot but also deep inside the target. In Ref. 4, for example, it was shown that when a silicon foil is irradiated by a PW laser pulse, the lines of the H- and He-like ions Si XIV and Si XIII are resonantly absorbed by the part of the target that does not interact directly with the laser radiation. This means that a plasma with a high content of these ions has formed there due to the transport of laser energy absorbed within the focal spot.

As a first approximation, it can be assumed that the generated plasma consists of two layers. The first is a high-temperature layer on the side of the target exposed to front laser irradiation. The second layer has a comparatively low temperature and is located on the back

of the target. The temperature of the first layer exceeds hundreds of electron volts at laser pulse intensities of 1×10^{14}–1×10^{21} W/cm^2 and is a source of comparatively hard x-ray radiation with $h\omega > 1$ keV. This radiation enables the determination of the layer's parameters using various approaches of x-ray spectroscopy diagnostics (see, e.g., Refs. 5–7). The second plasma layer has a much lower temperature, and approaches of x-ray emission diagnostics are not applicable to it. However, it can be diagnosed by detecting the spectral transmission of this layer. For this purpose, it is sufficient to register the x-ray spectrum of plasma created on the front side of the target $f(\lambda)$, i.e., the side irradiated by the laser, and the spectrum of plasma formed on the rear side of the target $r(\lambda)$. If the second plasma layer does not emit in the observed wavelength range, then the spectrum registered from the rear side is the spectrum emitted from the front layer and partially absorbed in the rear layer, i.e., $r(\lambda) = T(\lambda) \cdot f(\lambda)$, where $T(\lambda)$ is the spectral transmittance of the rear layer. The spectral transmittance is a function of plasma electron temperature T_e and the plasma electron density N_e in the rear layer and can be calculated using a kinetic code for radiative collisions that considers the effects of radiative transfer. By measuring the spectral transmittance and comparing it with the calculated results, the plasma parameters in the rear layer can be determined, as has been done for example in Ref. 4. In the experiments described here, an attempt was made to implement this approach when the foil target is additionally preheated from the rear side by a low-energy laser pulse. Experiments of this type are now of great interest in the context of accelerating laser particles in subcritical density plasma (created by a preheating pulse).[8–10] For example, the effect of selective ion acceleration in a collisionless shock was recently observed[11] with such a double-sided irradiation scheme.

Additional irradiation should increase the temperature on the rear side and thus shift the charge state distribution of the plasma toward more highly charged ions. This, in turn, should lead to a stronger suppression of these ion lines in the spectrum registered by the rear side of the target. The experimental observation of more efficient absorption of He-like ions by a preheated target, for example, is evidence that the rear side irradiation increases the temperature to values $\geq 1/4 \cdot IP_{Li}$, where IP_{Li} is the ionization potential of the corresponding Li-like ions. This is because, as estimates using the coronal kinetic model show for a variety of chemical elements (see, e.g., Ref. 12) at lower temperatures the number of He-like ions in the plasma is minimal, and the low-temperature layer practically does not absorb the spectral lines of He-like ions. Note that this conclusion for He-like chlorine ions is confirmed by our calculations in the framework of full radiative collision kinetics, which does not use the coronal approximation. However, the experimental studies carried out in this work for a chlorine-containing target have shown that a completely opposite situation may take place. It was observed that preheating may result in a decrease in resonant absorption coefficients.

The experiments were performed at the J-KAREN-P laser facility of the Kansai Institute for Photon Science (KPSI QST, Japan).[13,14] The general concept of the experiment is shown in Fig. 1(a). A 2-μm-thick foil made of C_8H_7Cl (4-chlorostyrene) was irradiated by a laser pulse ("main pulse") with duration $\tau \sim 40$ fs (FWHM) and wavelength $\lambda = 0.8\ \mu$m, focused on the target foil into a spot with a diameter $d \sim 2\ \mu$m. The pulse energy on the target reached $E_{las} \sim 12$ J. The listed values correspond to a laser intensity of $I_{lt} \sim 1 \times 10^{21}$ W/cm^2. The value of the temporal contrast was $K_{las} \sim 1 \times 10^{10}$. For some shots (referred below as "double-sided"), the foil was preheated (2.5 ns before the main pulse) by a low energy (1% of E_{las}) "prepulse" focused into a 300 μm spot on the rear side of the target. Durations of the main pulse and "prepulse" were the same. Since the "prepulse" energy was 2 orders of magnitude lower than the main pulse energy, and the intensity was 6 orders of magnitude lower, the preheating could not significantly change the properties of the radiating front layer. Its task was, first, to increase the temperature of the rear region, and, second, to increase the velocity of its expansion v_0.

Spectra of radiation emitted from the rear side of the foil were registered by Focusing Spectrometers with Spatial Resolution (FSSR).[15] The FSSR was installed at a distance of $l = 2295$ mm from the source, at an angle of $\sim 35°$ to the laser axis in the horizontal plane and 23.1° in the vertical plane. The spectrometer was equipped with a spherically bent α-quartz crystal 1011 ($R = 150$ mm is the radius of curvature, $2d = 6.666$ Å is the interplanar distance) and was configured to observe the wavelength range 3.7–4.3 Å with spectral resolution of $\lambda/\Delta\lambda \sim 3000$. The range contains a resonant doublet of the Cl H-like ion $Ly_{\alpha 1,2}$ ($\lambda_1 = 4.1852$ Å, $\lambda_2 = 4.1906$ Å), a group of dielectronic satellites with characteristic wavelengths of 4.22–4.25 Å, and the He_β line ($\lambda = 3.7894$ Å). An Andor DX-440 CCD camera (pixel size 13.5 μm) was used as an x-ray detector. The camera sensor was protected from the visible radiation by a filter consisting of two layers of polypropylene (C_3H_6, thickness 1 μm) with a 0.2 μm thick Al coating. The spectra were recorded in single-shot mode. The raw data were corrected according with transmission of the filter foils, crystal reflectivity and quantum efficiency of the x-ray detectors as described in the Appendix of Ref. 18. Examples of spectra registered with and without preheating are shown in Fig. 1(b).

It is necessary to underline that the measured spectra showed high shot-to-shot reproducibility. The peak intensity ratio between He_β and Ly_α lines was equal to 0.77 (± 0.05) in all fourteen shots under preheating of the back side of the target and equal to 0.24 (± 0.02) in all seventeen shots with front side target irradiation only.

As seen from the figure, preheating leads to an increase in the intensity of the He_β line and at the same time does not influence the Ly_α intensity. In the following, it is shown that such an effect can occur due to shift [Fig. 2(c)] in the absorption bands of the matter on the target's rear side due to its high velocity of movement relative to the emitting hot plasma on the front side. To explain the effect in detail, it should first be discussed what exactly is registered by the spectrometer when it is installed from the rear side of the foil.

In general, it is the sum of the contributions of radiation emitted by (1) relatively cold plasma forming on the rear side of the target and (2) hot plasma from the front side. The latter is also partially absorbed by the cold plasma before it reaches the spectrometer. The maximum degree of ionization Q_c in the cold plasma is lower. Therefore, if the spectrometer on the rear side is set to register the lines emitted by ions with $> Q_c$, then the registered spectrum is actually the spectrum of the hot plasma from the front side, weakened by non-resonant absorption by the rear side cold plasma. Of course, dividing the plasma volume into two parts is a rough approximation, but as shown in Ref. 4, it works well and allows to retrieve physically relevant diagnostic results.

The transmission calculations for a stationary plasma were performed with the detailed radiation collision code PrismSPECT,[16,17] which takes into account the effects of self-absorption of spectral lines within the Biberman–Holstein escape factor.[12] Since the prepulse was

focused in a large spot with a diameter of 300 μm, the expansion of the rear plasma can be considered as flat over distances of the order of the focal spot size. In this case, the plasma transmission is independent of time, since the product $S = h \cdot N_i$, which determines it, is a constant. Since at the initial time, $h = 2\ \mu$m, and the ion density is equal to the Cl solid $N_i = 7.6 \times 10^{22}$ cm^{-3}, the value $S = 1.52 \times 10^{18}$ cm^{-2} was used for calculations. The spectral transmission initially calculated for a stationary plasma was then shifted by the Doppler shift in the wavelength. Note that at expansion velocities of $\sim 1 \times 10^8$ cm/s, the rear plasma expands in 2.5 ns to distances of about 2.5 mm. In this case, the expansion can no longer be considered flat. This leads to parameter S becoming smaller, as the density decreases faster than 1/h. This in turn leads to an increase in the spectral transmission of plasma. However, since resonant absorption of spectral lines is impossible at such velocities of motion, due to the different positions of the emission and absorption lines, this has no influence on the calculation of the spectrum measured from the rear side.

Nevertheless, the heating of the rear side of the target by the main front laser pulse becomes increasingly effective as the foil thickness decreases. It means the temperature values of the rear "cold" and the front "hot" plasma should be quite close to each other for thin targets.

In this case, the rear side spectrometer registers the spectrum of the high-temperature plasma layer with a thickness h (~ thickness of the foil). Its shape can be influenced by self-absorption. The degree of influence depends on the h value. It can be insignificant, but should always be checked carefully. Unjustified exclusion of self-absorption from consideration can lead to incorrect diagnostic results. It can be demonstrated based on the experimental spectrum registered without preheating. As it described in Refs. 18–20 it is possible to determine the electron density N_e and the temperature T_e of the plasma from the shape of the Ly_α and its dielectronic satellites. The shape of these lines was simulated with the radiation collision code PrismSpect[16] for different values of (N_e, T_e) and compared with the experiment. Significantly, the lines used in this diagnostic approach are not absorbed in the rear plasma layer, because the lower levels of the satellites are excited states of He-like ions, and the number of H-like ions in the rear layer is small. Although the calculations were performed for density and temperature values that vary over a wide range, Figs. 2(a) and 2(b) show only the results closest to the experimental ones. In the radiative collision calculations, a large number of levels belonging to chlorine ions ranging from F-like to H-like were considered, and the fine structure of all states was included. Ions from Cl-like to Ne-like were not included, as they do not contribute to the emitted spectrum

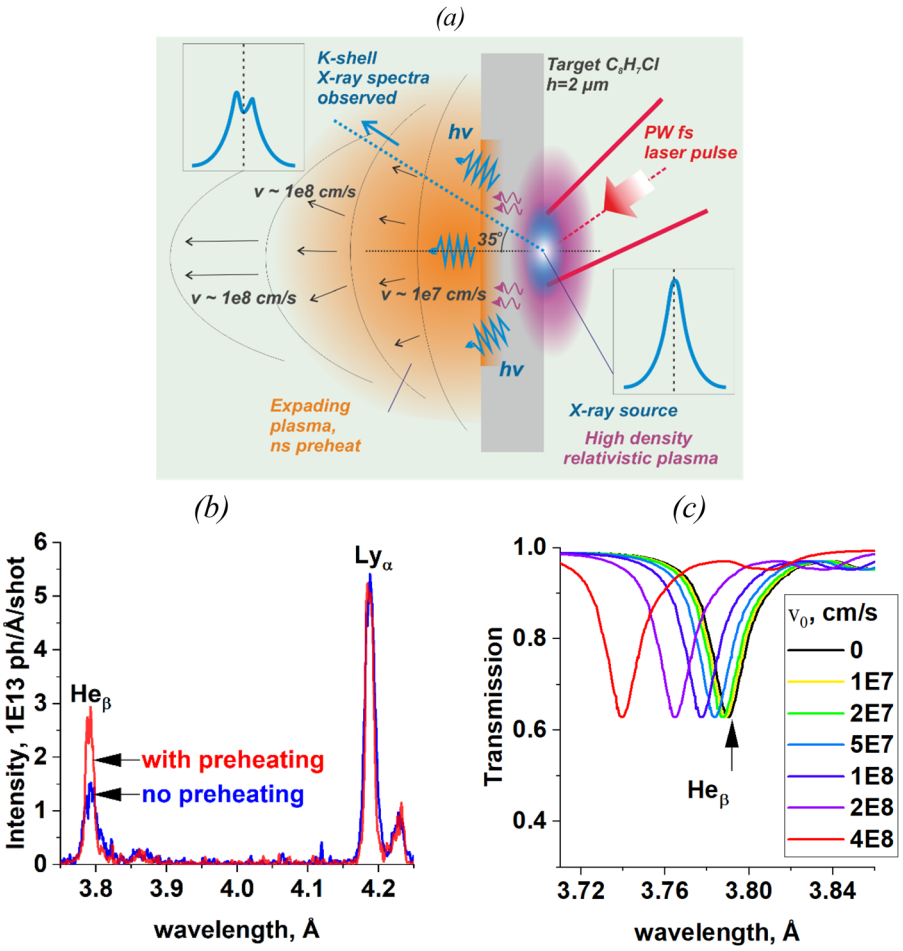

FIG. 1. (a) General scheme of the experiment on double-sided C_8H_7Cl foil irradiation; (b) K-shell x-ray spectra observed for single-sided ("no preheating") and double-sided (with preheating) irradiation; (c) dependence of C_8H_7Cl plasma transmission in the He_β line wavelength range on its velocity of movement in the direction of the observer v_0. The calculation was performed assuming a flat expansion of a plasma layer with a thickness of $h = 2\ \mu$m and a solid-state ion density of the plasma $N_i = 7.6 \times 10^{22}$ cm^{-3}.

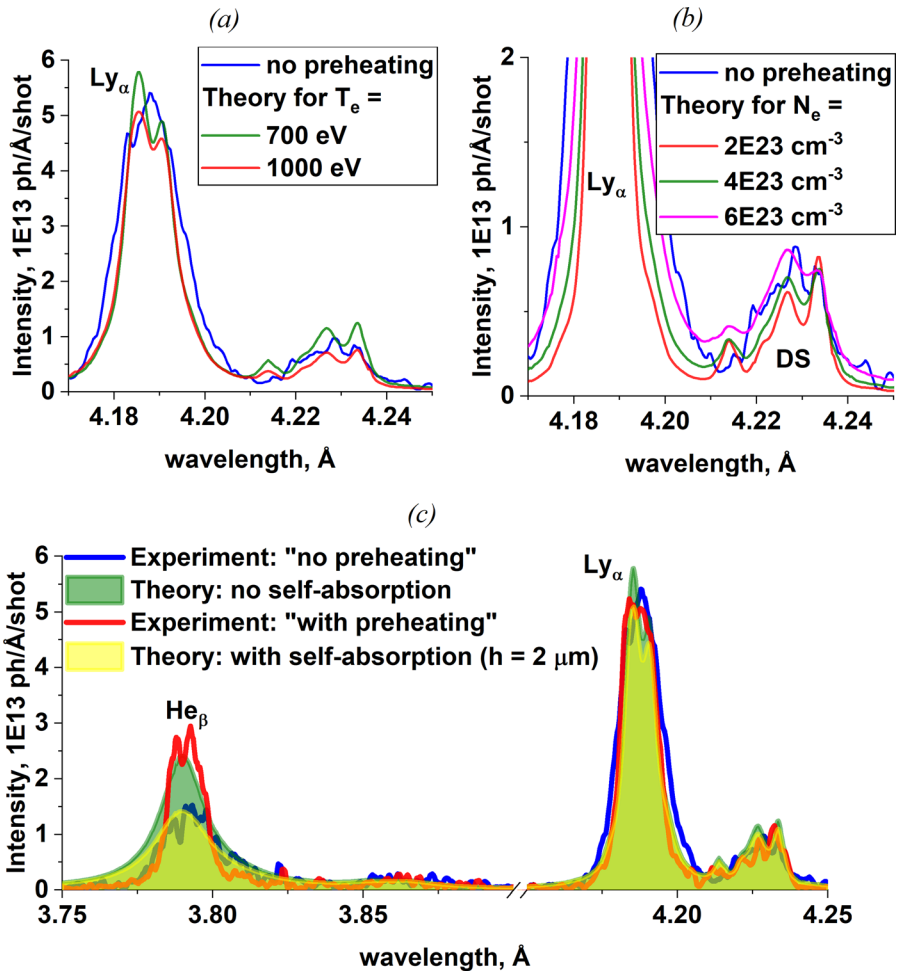

FIG. 2. Comparison of the experimental spectrum registered for "no preheating" case and the theoretical spectra simulated for (a) fixed ion density Ni = 7.6×10^{22} cm^{-3} and two different Te; (b) fixed Te = 800 eV and different electron densities Ne; (c) comparison of experimental spectra registered for single- and double-sided irradiation ("with preheating") and the theoretical ones simulated for fixed Te = 700 eV and Ne = 3.5×10^{23} cm^{-3} with and without self-absorption. In pictures (a)–(c) in the case "with self-absorption" it was assumed that plasma is a flat layer with thickness h = 2 μm. The break for (c) is from 3.9 to 4.15 Å.

in the spectral range considered. The code included both collisionless (radiative decay, autoionization, photoionization) and collisional (dielectronic capture, excitation and de-excitation by electron impact, ionization and triple recombination) processes, as well as self-absorption effects (Biberman–Holstein approximation). Comparison [Figs. 2(a) and 2(b)] shows that parameters of the plasma created in the experiment were 700 eV$\leq$ T$_e$ $\leq$ 1000 eV and 3.5×10^{23} cm^{-3} $\leq$ N$_e$ $\leq$ 5.5×10^{23} cm^{-3}. For example, the spectrum simulated for T$_e$ = 700 eV and N$_e$ = 3.5×10^{23} cm^{-3} agrees well with the experimental one [blue line in Fig. 2(c)] registered for the "no preheating" case across the observed range, only when self-absorption was considered [yellow line in Fig. 2(c)]. The results of the simulation for the same values of N$_e$ and T$_e$, but without self-absorption [green line in Fig. 2(c)], do not reproduce the experimental shape of the He$_\beta$ line.

On the other hand, it corresponds much better to the form of He$_\beta$ observed for the case of preheating [red line in Fig. 2(c)]. This leads to one of the possible explanations for the increase in He$_\beta$ intensity observed for double-sided irradiation: in some way, preheating makes the produced plasma optically thin for this line. The only possible mechanism is related to the macroscopic relative motion of the plasma regions. It can significantly reduce the influence of self-absorption on the shape of the emission lines. If two plasma regions move relative to each other with velocity v$_0$, the absorption coefficient of one for the line with center in ω_0 emitted by the other is proportional to f(ω_0(1+v$_0$/c)) instead of f(ω_0). Even for small values of v$_0$, f(ω_0 (1+v$_0$/c)) can be significantly lower than f(ω_0). With increasing velocities, the overlap of the absorption contour f(ω_0 (1+v$_0$/c)) and the emission contour f(ω_0) becomes smaller. For ω_0v$_0$/c $\gg$ $\Delta\omega_0$, where $\Delta\omega_0$ is the natural width of the line, they do not overlap at all, so the plasma becomes optically thin. Numerical estimates of the effect were made for the C_8H_7Cl plasma generated in the experiment [Fig. 1(c)]. The figure shows that when the velocity of the relative motion of the emitting and absorbing plasma is around 3×10^8 cm/s, the absorbing plasma becomes almost transparent to the lines of He-like Cl XVI ions. If the emission and absorption profiles only partially overlap, the transparency is partial. For example, Fig. 3 shows the results of the calculations of the spectra that should be registered by the rear side spectrometer during double-sided irradiation if it is assumed that an emitting plasma with T$_e$ = 700 eV appears on the front side and an absorbing plasma with T$_e$ = 400 eV on the rear side. For the calculations, it was assumed that the electron density for both plasmas is N$_e$ = 3.5×10^{23} cm^{-3} and that the thickness of the rear

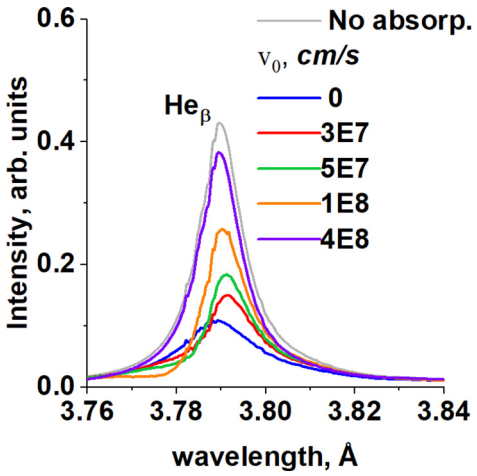

FIG. 3. The calculated Cl He_β line profile which should be registered from the rear side of the target, depending on the relative velocity of the plasmas – v_0.

plasma is 6 μm. It can be clearly seen that both the shape of the profile and the intensity of the He_β line are very sensitive to the velocity of relative motion, which can be used to measure this plasma expansion parameter.

DISCUSSION

If parts of the plasma move relative to each other at high velocity, the effect of partial or complete transparency can occur due to the Doppler effect. This means that a spectral line emitted by one part is only weakly or not at all absorbed by the other part, even if it contains ions that can absorb the line resonantly at zero relative velocity. It can be the case, for example, if the plasma is generated by irradiating the film with two laser pulses from the front and rear. In this case, there are two plasma regions (rear and front). Depending on the parameters of the irradiation lasers, they can have very similar or completely different temperatures and densities, but the most important thing is that they expand in opposite directions. As a result, the velocity of their relative motion v_0 is the sum of their own velocities. Their values should be $\sim 1 \times 10^8$ cm/s at the intensities used in our experiments. This plasma velocity is estimated from the observed spectral linewidth, which is of the order of $\Delta\lambda \sim 0.01$–0.02 Å. Since the linewidth is mainly due to the Doppler broadening associated with the macroscopic motion of the plasma, $v_0 \sim c(\Delta\lambda/\lambda) \sim (1\text{–}2) \times 1 \times 10^8$ cm/s. As a result, the plasmas on the back side should become transparent to the spectral lines emitted from the front side. In this work, it was observed experimentally for the He_β line of the Cl He-like ion.

At the same time, the transparency effect should not occur with one-sided irradiation. Since in this case hot (outer) and warm (inner) layers move mainly in one direction, the relative velocity v_0, which is calculated as the difference between the velocities of the two layers, should not be higher than 10^7 cm/s. The results of our experiments show that even the intensity of $\sim 1 \times 10^{21}$ W/cm^2 is not sufficient to provide v_0 value for the transparency effect to occur. In this case, the parameters of the inner plasma can be determined by the method of absorption spectroscopy according to Ref. 4.

CONCLUSION

In conclusion, we demonstrated velocity-dependent self-absorption in x-ray spectra of thin foils: When the foils are irradiated by laser pulses from both sides, the doppler shift leads to absence of resonance absorption of the chlorine He_β line observed through the expanding foil.

ACKNOWLEDGMENTS

The work of I. Yu., M.A., S.N., and R.K. was supported by the Russian Science Foundation (Project No. 25-42-00011, https://rscf.ru/en/project/25-42-00011/); The work also supported by Japan Society for the Promotion of Science (JSPS) KAKENHI Grants No. JP25H00622, No. JP15H02154, No. JP17H06202, No. JP22H00119 and JSPS Core-to-Core Program B. Asia-Africa Science Platforms Grant No. JPJSCCB20190003.

AUTHOR DECLARATIONS

Conflict of Interest

The authors have no conflicts to disclose.

Author Contributions

I. Yu. Skobelev: Conceptualization (equal); Data curation (equal); Investigation (equal); Methodology (equal); Writing – original draft (equal). **M. A. Alkhimova:** Conceptualization (equal); Data curation (equal); Formal analysis (equal); Investigation (equal); Writing – original draft (equal). **T. Pikuz:** Data curation (supporting); Formal analysis (supporting); Investigation (equal); Writing – original draft (supporting). **S. N. Ryazantsev:** Data curation (equal); Formal analysis (equal); Investigation (equal); Writing – original draft (equal). **R. K. Kulikov:** Data curation (supporting); Formal analysis (supporting). **A. Sagisaka:** Investigation (equal); Writing – review & editing (supporting). **K. Ogura:** Investigation (equal); Methodology (supporting); Resources (supporting). **Ko. Kondo:** Formal analysis (supporting); Investigation (equal); Methodology (supporting). **Y. Miyasaka:** Investigation (equal); Methodology (supporting). **M. Nishikino:** Formal analysis (supporting); Investigation (equal). **M. Kando:** Investigation (equal); Project administration (equal); Resources (lead); Software (supporting); Supervision (supporting); Validation (supporting); Writing – review & editing (supporting). **H. Kiriyama:** Investigation (equal); Methodology (supporting); Resources (equal); Software (lead); Supervision (supporting); Validation (supporting). **A. S. Pirozhkov:** Investigation (equal); Resources (supporting); Software (supporting); Writing – review & editing (supporting). **K. Kondo:** Funding acquisition (supporting); Investigation (supporting); Project administration (equal); Supervision (equal); Validation (supporting). **M. Ota:** Investigation (supporting); Resources (supporting). **S. Egashira:** Investigation (supporting); Methodology (supporting); Resources (supporting). **T. Minami:** Investigation (supporting); Software (equal). **S. Jinno:** Formal analysis (equal); Investigation (equal); Resources (equal). **M. Kanasaki:** Investigation (equal); Methodology (supporting); Resources (supporting). **Y. Kuramitsu:** Formal analysis (supporting); Investigation (lead); Project administration (equal); Resources (supporting); Supervision (supporting); Writing – review & editing (supporting). **T. Kawachi:** Formal analysis (supporting); Investigation (equal). **R. Kodama:** Funding acquisition (supporting); Investigation

(supporting); Project administration (equal); Software (supporting); Supervision (equal); Validation (equal). **Y. Fukuda:** Conceptualization (supporting); Formal analysis (supporting); Investigation (equal); Resources (equal); Supervision (supporting); Validation (supporting); Writing – review & editing (equal). **S. Pikuz:** Conceptualization (supporting); Formal analysis (supporting); Supervision (equal); Validation (equal); Writing – review & editing (equal). **Y. Sakawa:** Conceptualization (equal); Funding acquisition (equal); Investigation (lead); Project administration (lead); Software (supporting); Supervision (equal).

DATA AVAILABILITY

The data that support the findings of this study are available from the corresponding author upon reasonable request.

REFERENCES

[1]M. Honda, J. Meyer-ter-Vehn, and A. Pukhov, "Two-dimensional particle-in-cell simulation for magnetized transport of ultra-high relativistic currents in plasma," Phys. Plasmas **7**(4), 1302–1308 (2000).

[2]V. T. Tikhonchuk, "Interaction of a beam of fast electrons with solids," Phys. Plasmas **9**(4), 1416–1421 (2002).

[3]A. R. Bell, J. R. Davies, S. Guerin, and H. Ruhl, "Fast-electron transport in high-intensity short-pulse laser - solid experiments," Plasma Phys. Controlled Fusion **39**(5), 653–659 (1997).

[4]I. Y. Skobelev, S. N. Ryazantsev, D. D. Arich, P. S. Bratchenko, A. Y. Faenov, T. A. Pikuz, P. Durey, L. Doehl, D. Farley, C. D. Baird, K. L. Lancaster, C. D. Murphy, N. Booth, C. Spindloe, P. McKenna, S. B. Hansen, J. Colgan, R. Kodama, N. Woolsey, and S. A. Pikuz, "X-ray absorption spectroscopy study of energy transport in foil targets heated by petawatt laser pulses," Photonics Res. **6**(4), 234 (2018).

[5]H. J. Kunze, *Introduction to Plasma Spectroscopy* (Springer Science & Business Media, 2009).

[6]M. Schnürer, M. P. Kalashnikov, P. V. Nickles, T. Schlegel, W. Sandner, N. Demchenko, R. Nolte, and P. Ambrosi, "Hard x-ray emission from intense short pulse laser plasmas," Phys. Plasmas **2**(8), 3106–3110 (1995).

[7]L. P. Presnyakov, "X-ray spectroscopy of high-temperature plasma," Sov. Phys. Usp. **19**(5), 387–399 (1976).

[8]R. Kumar, Y. Sakawa, L. N. K. Döhl, N. Woolsey, and A. Morace, "Enhancement of collisionless shock ion acceleration by electrostatic ion two-stream instability in the upstream plasma," Phys. Rev. Accel. Beams **22**(4), 043401 (2019).

[9]W. Zhang, H. Cai, and S. Zhu, "The formation and dissipation of electrostatic shock waves: The role of ion–ion acoustic instabilities," Plasma Phys. Controlled Fusion **60**(5), 055001 (2018).

[10]H. B. Zhuo, Z. L. Chen, Z. M. Sheng, M. Chen, T. Yabuuchi, M. Tampo, M. Y. Yu, X. H. Yang, C. T. Zhou, K. A. Tanaka, J. Zhang, and R. Kodama, "Collimation of energetic electrons from a laser-target interaction by a magnetized target back plasma preformed by a long-pulse laser," Phys. Rev. Lett. **112**(21), 215003 (2014).

[11]Y. Sakawa, H. Ishihara, S. N. Ryazantsev, M. A. Alkhimova, R. Kumar, O. Kuramoto, Y. Matsumoto, M. Ota, S. Egashira, Y. Nakagawa, T. Minami, K. Sakai, T. Taguchi, H. Habara, Y. Kuramitsu, A. Morace, Y. Abe, Y. Arikawa, S. Fujioka, M. Kanasaki, T. Asai, T. Morita, Y. Fukuda, S. Pikuz, T. Pikuz, Y. Ohira, L. N. K. Döhl, N. Woolsey, and T. Sano, "Laser-driven proton-only acceleration in a multicomponent near-critical-density plasma," Phys. Rev. Lett. **133**(19), 195102 (2024).

[12]E. A. Y. Igor, I. Sobel'man, L. A. Vainshtein, and E. A. Yukov, *Excitation of Atoms and Broadening of Spectral Lines* (Springer, Berlin, 1995).

[13]H. Kiriyama, Y. Miyasaka, A. Sagisaka, K. Ogura, M. Nishiuchi, A. S. Pirozhkov, Y. Fukuda, M. Kando, and K. Kondo, "Experimental investigation on the temporal contrast of pre-pulses by post-pulses in a petawatt laser facility," Opt. Lett. **45**(5), 1100 (2020).

[14]A. S. Pirozhkov, Y. Fukuda, M. Nishiuchi, H. Kiriyama, A. Sagisaka, K. Ogura, M. Mori, M. Kishimoto, H. Sakaki, N. P. Dover, K. Kondo, N. Nakanii, K. Huang, M. Kanasaki, K. Kondo, and M. Kando, "Approaching the diffraction-limited, bandwidth-limited Petawatt," Opt. Express **25**(17), 20486 (2017).

[15]A. Y. Faenov, S. A. Pikuz, A. I. Erko, B. A. Bryunetkin, V. M. Dyakin, G. V. Ivanenkov, A. R. Mingaleev, T. A. Pikuz, V. M. Romanova, and T. A. Shelkovenko, "High-performance x-ray spectroscopic devices for plasma microsources investigations," Phys. Scr. **50**(4), 333–338 (1994).

[16]J. J. MacFarlane, I. E. Golovkin, P. R. Woodruff, S. K. Kulkarni, and I. M. Hall, "Simulation of plasma ionization and spectral properties with PrismSPECT," in *Abstracts IEEE International Conference on Plasma Science* (IEEE, 2013), p. 1.

[17]See https://Prism-Cs.Com/Software/PrismSPECT/Overview.Html for "PrismSPECT."

[18]S. N. Ryazantsev, A. S. Martynenko, M. V. Sedov, I. Y. Skobelev, M. D. Mishchenko, Y. S. Lavrinenko, C. D. Baird, N. Booth, P. Durey, L. N. K. Döhl, D. Farley, K. L. Lancaster, P. McKenna, C. D. Murphy, T. A. Pikuz, C. Spindloe, N. Woolsey, and S. A. Pikuz, "Absolute keV x-ray yield and conversion efficiency in over dense Si sub-petawatt laser plasma," Plasma Phys. Controlled Fusion **64**(10), 105016 (2022).

[19]I. I. Sobel'Man, *Introduction to the Theory of Atomic Spectra* (Elsevier, 1972).

[20]A. S. Martynenko, I. Y. Skobelev, S. A. Pikuz, S. N. Ryazantsev, C. Baird, N. Booth, L. Doehl, P. Durey, D. Farley, R. Kodama, K. Lancaster, P. McKenna, C. Murphy, C. Spindloe, T. A. Pikuz, and N. Woolsey, "Determining the short laser pulse contrast based on X-Ray emission spectroscopy," High Energy Density Phys. **38**, 100924 (2021).